Statistical Integration of Time-lapse Seismic and Electromagnetic Data for Reservoir Monitoring and Management

Jaehoon Lee[1], Tapan Mukerji[1] and Michael Tompkins[2]
[1]Department of Energy Resources Engineering, Stanford University
[2]PolytopX

Abstract

Joint integration of seismic and electromagnetic (EM) data can improve the quality of characterization of hydrocarbon reservoirs because these two types of measurement are based on fundamentally different physics so they are sensitive to different reservoir properties. In this work, we extended this advantage in reservoir monitoring by jointly integrating time-lapse seismic and EM data. One of the possible ways of combining two data sources is statistical integration, where the joint and conditional probability density functions (PDF) of seismic and EM data, as well as reservoir properties, need to be modeled. However, there is a critical issue of the scale differences between well logs, seismic, and EM data since each of them represents different volumes of a reservoir.

In this research, we established a workflow to statistically integrate time-lapse seismic and EM data by developing a proper and efficient method to upscale the joint PDFs considering the scale differences. In the developed PDF upscaling method, geologically analogous reservoirs to the target reservoir are generated by unconditional multipoint geostatistical simulation, SNESIM (Strebelle, 2000; 2002). Well-scale seismic and EM attributes are randomly assigned to the analogous reservoirs using conditional PDFs given facies obtained from well log analysis. Forward modeling and inversion of the analogous reservoirs or appropriate filtering provides field-scale seismic and EM data. Multivariate (tri-variate for reservoir characterization and hexa-variate for time-lapse monitoring) PDFs are constructed with nonparametric or parametric (Gaussian mixture) assumptions.

We tested this approach in classifying facies; oil sand, brine sand, and shale of a synthetic reservoir. We found that the significantly improved classification with simulated field-scale joint PDFs was achieved compared to that with well-scale PDFs. Also, joint integration of seismic and EM data provided substantial advantages for facies classification over the one obtained from the separate use of seismic and EM data.

Introduction

Continuous data gathering and monitoring are an important aspect of reservoir management in order to maximize hydrocarbon recovery because a reservoir continuously changes its state and contents as it is depleted. Time-lapse (4D) seismic monitoring has been used to keep track of changes due to production in many fields (e.g., Tura and Lumley, 1999; Landrø, 2001; Lumley et al., 2003). However, large differences enough to be detectable by seismic measurements usually occur when hydrocarbon recovery in reservoirs considerably alters the elastic properties of the mixture of pore fluids and reservoir rocks are not too stiff to be in sensitive to changes in pore fluids.

Electromagnetic (EM) techniques (Alumbaugh and Morrison, 1995; Constable and Cox, 1996) also have been attempted as key tools for reservoir monitoring. Electrical contrast obtained by EM methods can provide a useful means of monitoring the fluid changes in reservoirs even when 4D seismic differences are not significant. The resolution of EM methods, however, is generally not as good as seismic measurements by themselves.

In recent years, many researchers (e.g., Hoversten et al., 2006; Gao et al., 2012) have addressed joint integration of multidisciplinary geophysical data for better reservoir characterization because different geophysical data can give complementary information on reservoir properties. The advantages of joint integration of different geophysical data in reservoir characterization can also be gained in reservoir monitoring by jointly integrating time-lapse seismic and EM data.

In this research, we suggest statistical integration workflow with a new upscaling scheme, which simulates the joint probability density functions (PDF) of field-scale seismic and EM data as well as reservoir properties. The conceptual basis of the developed method is that successful results can be expected when reservoir properties are estimated from the field-scale PDFs of very analogous reservoirs to the target reservoir. Therefore, geologically analogous reservoirs are generated using unconditional multipoint geostatistical simulation, SNESIM (Strebelle, 2000; 2002) and well log analysis. Field-scale data of the analogous reservoirs are obtained by forward modeling and inversion techniques or filtering.

Theoretical Background

Multivariate probability distribution of reservoir properties and secondary data (seismic and EM data) can be utilized to assess the probability of discrete (facies) or continuous (fluid saturation or porosity) reservoir properties conditional to secondary data. This technique has been used in

seismic reservoir characterization (e.g., Avseth et al., 2000; Mukerji et al., 2001). The joint probability distribution of facies C and multiple secondary data Y can be defined as:

$$P(C, Y_1, \ldots, Y_n) \tag{1}$$

Once the joint probability distribution is modeled, a conditional probability of facies given seismic and EM data at a certain location in a reservoir is derived by the definition of a conditional probability:

$$P(C|Y_1 = y_1, \ldots, Y_n = y_n) = \frac{P(C, Y_1 = y_1, \ldots, Y_n = y_n)}{P(Y_1 = y_1, \ldots, Y_n = y_n)} \tag{2}$$

According to the Bayes' rule, the conditional probability of facies given secondary data can be denoted as:

$$P(C|Y_1 = y_1, \ldots, Y_n = y_n) \propto P(C) P(Y_1 = y_1, \ldots, Y_n = y_n|C) \tag{3}$$

If we assume that the occurrence of facies is a prior the same or do not know any prior information, facies classification can be made by the maximum likelihood as follows:

$$C = c_i \quad if \quad P(Y_1 = y_1, \ldots, Y_n = y_n|C = c_i) = maximum \tag{4}$$

Synthetic Example

A two-dimensional cross section is chosen from the three-dimensional synthetic reservoir, Stanford VI-E (Lee and Mukerji, 2012) that includes time-lapse seismic attributes and electrical resistivity. Three facies; oil sand, brine sand, and shale are determined based on saturation and mineralogy (Figure 1). Two vertical wells, indicated as red lines in the figure, are assumed.

Various empirical formulae are used to create point-scale (well-scale) velocities (Gardner et al., 1974; Castagna et al., 1985; 1993; Avseth et al., 2005) and electrical resistivity (Archie, 1942; Waxman and Smits, 1968). The details of the formulae can be found in the Stanford VI-E paper (Lee and Mukerji, 2012). In order to make field-scale seismic and EM data, Born filtering (Mukerji et al., 1997) is applied for seismic impedances and geometric moving average for electrical resistivity. Figure 2 shows the field-scale acoustic and elastic impedances and electrical resistivity of the synthetic example. These are assumed as inversion results of the target cross section shown in Figure 1. Figure 3 presents well logs at two vertical wells.

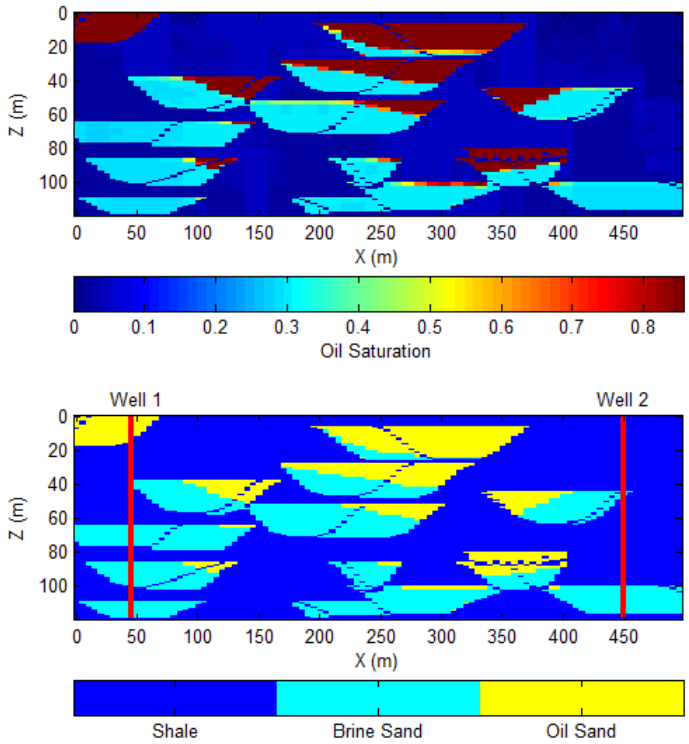

Figure 1. Two-dimensional synthetic cross section; oil saturation (top) and facies (bottom). Red lines indicate two vertical wells.

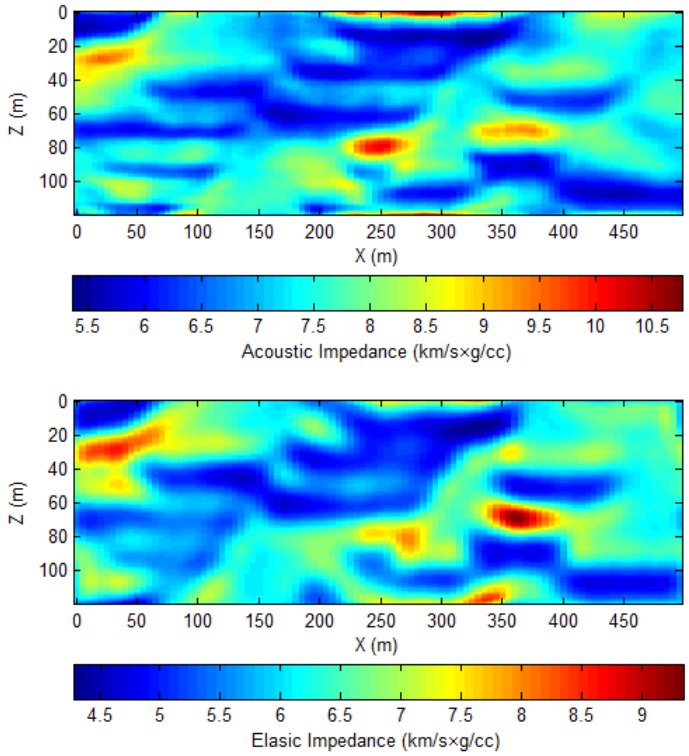

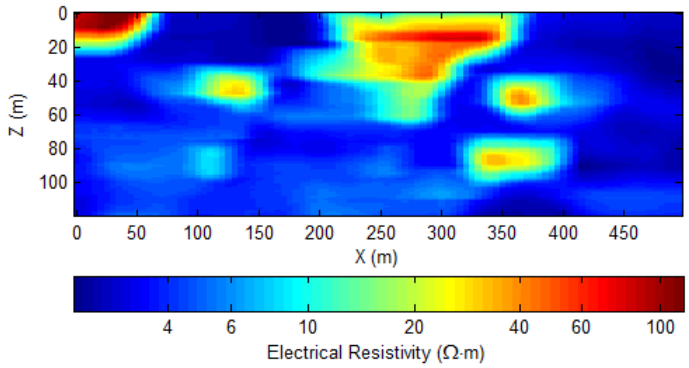

Figure 2. Seismic and electromagnetic data of the synthetic cross section; acoustic impedance (top), elastic impedance (30°) (middle), and electrical resistivity (bottom).

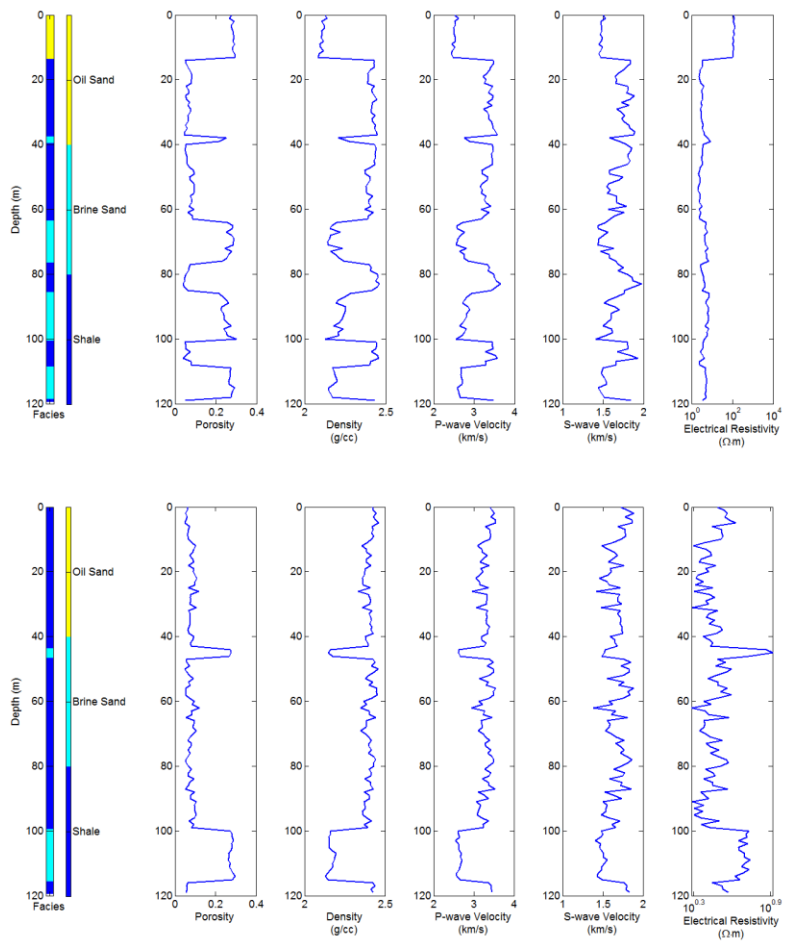

Figure 3. Well logs at two vertical wells in the synthetic cross section; well 1 (top) and well 2 (bottom).

Methodology

Figure 4 summarizes the procedure of multivariate probability distribution modeling with a new upscaling scheme to simulate the field-scale PDF of reservoir properties, seismic and EM data. First of all, well logs, such as facies, porosity, seismic velocities, and resistivity, are obtained from several wells. Well log data are then extended by rock physics modeling and Monte Carlo simulation to possible values in the reservoir but not encountered in the wells; e.g. values for possible porosity and saturation. Well-scale joint PDF is computed from the extended well log data.

Now geologically analogous reservoirs to the target reservoir are generated by multipoint geostatistical algorithm, SNESIM. Note that we are just trying to simulate the field-scale PDF, and not doing sampling or matching data, so we need only a few realizations using unconditional simulation. In this example, three realizations are used (Figure 6).

Well-scale seismic and EM attributes given facies are randomly assigned to the analogous reservoirs using the well-scale PDF obtained from well log analysis. The same forward modeling and inversion techniques used for the target reservoir are applied to get the field-scale data of the analogous reservoirs. Alternatively, appropriate filters, induced from comparison with the result of forward modeling and inversion, can be applied for quick simulation of field-scale data. The field-scale PDF of the analogous reservoirs, finally, can be calculated with nonparametric or parametric assumptions (Gaussian mixture) because all the information is known everywhere of analogous reservoirs. Therefore, the obtained PDF is (see Figure 4):

$$P\left(C, AI_{field}, EI_{field}, R_{field}\right) \tag{5}$$

where AI_{field} and EI_{field} are, respectively, field-scale acoustic and elastic impedances, R_{field} is electrical resistivity

The same procedure is applied to integrate time-lapse seismic and EM data into the joint PDF. The difference is that we need two different saturation profiles for each realization. When well-scale data are assigned at the same location for different saturations, they should be somewhat related to each other otherwise the simulated PDF does not reflect the changes in the reservoir properly. Therefore, we first assign porosity given facies to the analogous reservoirs, and then seismic impedances and electrical resistivity given facies and porosity using the well-scale PDF. This is based on the assumption that porosity does not change much during production. The obtained PDF is:

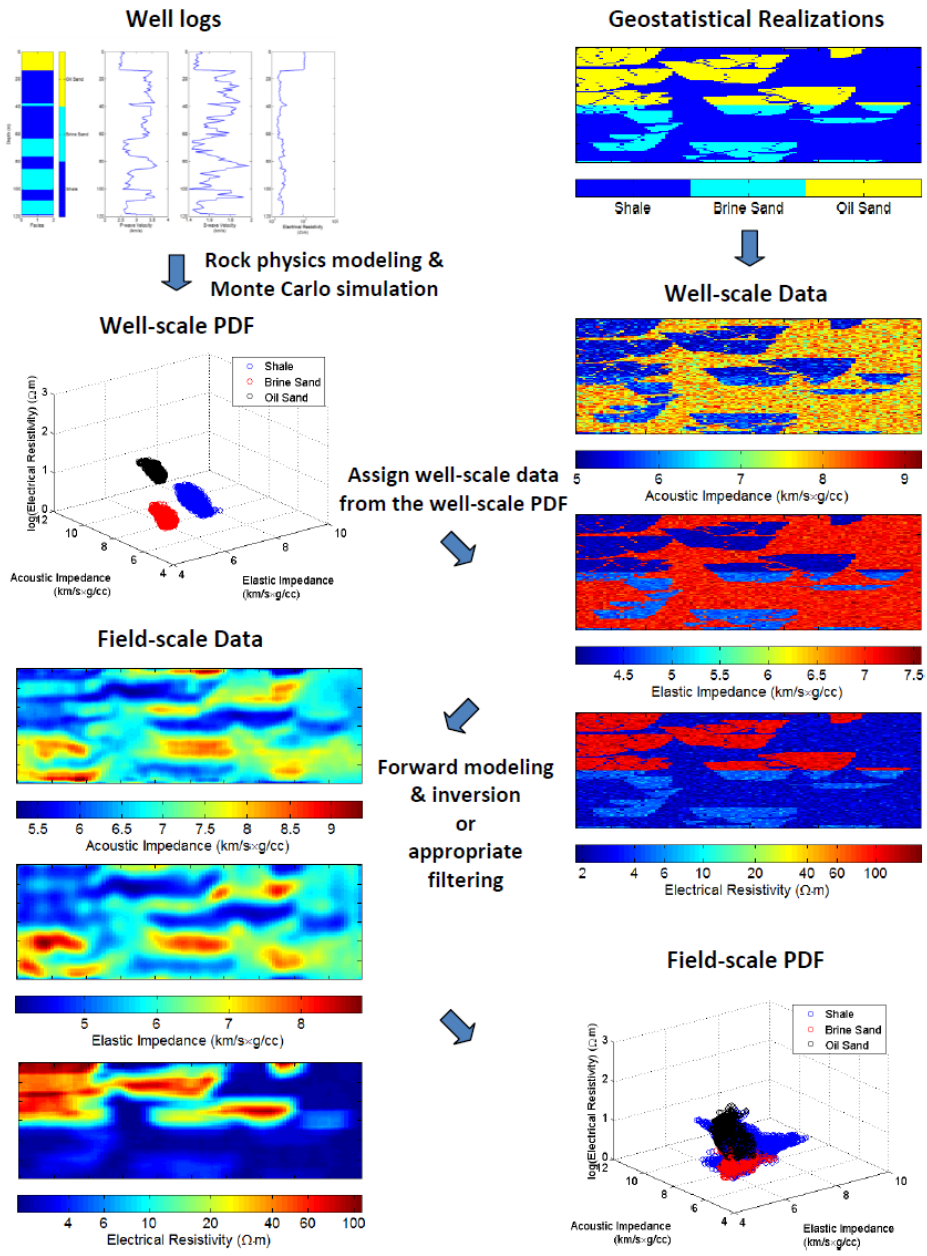

Figure 4. Procedure of statistical integration of seismic and electromagnetic data with a PDF upscaling method.

$$P\left(C, AI_{field}^{t-1}, EI_{field}^{t-1}, R_{field}^{t-1}, AI_{field}^{t}, EI_{field}^{t}, R_{field}^{t}\right) \tag{6}$$

where subscripts t and t-1 denote two measurements at different times during production.

From multiple applications to time-lapse data, it was concluded that nonparametric modeling is not well applicable to time-lapse monitoring since a hexa-variate PDF given facies requires too many data. On the other hand, a Gaussian mixture model gives satisfactory results with a fair amount of data. Also, it gives better results when seismic and EM data at the previous time step are incorporated into the joint PDF than differences of those attributes between two different time steps. This is because the differences of attributes are not purely physical properties, also related to production. Differences can be similar in undepleted regions regardless of facies; thus it can deteriorate classification.

Results

Seismic impedances and electrical resistivity, which are obtained from well logs (Figure 3), are presented in Figure 5. The extended data by rock physic modeling and Monte Carlo simulation are also plotted with well log data.

Figure 6 shows three realizations that are generated by unconditional multipoint geostatistical algorithm as analogous reservoirs to the target cross section. Well-scale seismic impedances and electrical resistivity given facies are assigned to these realizations using the extended well log data shown in Figure 5. Field-scale data are obtained through the forward modeling and inversion techniques used for the target reservoir or appropriate filtering. In this synthetic example, the same Born filtering and the geometric moving average are applied to the generated realizations as to the target cross section. Figure 7 presents well-scale and field-scale seismic impedances and electrical resistivity of three realizations.

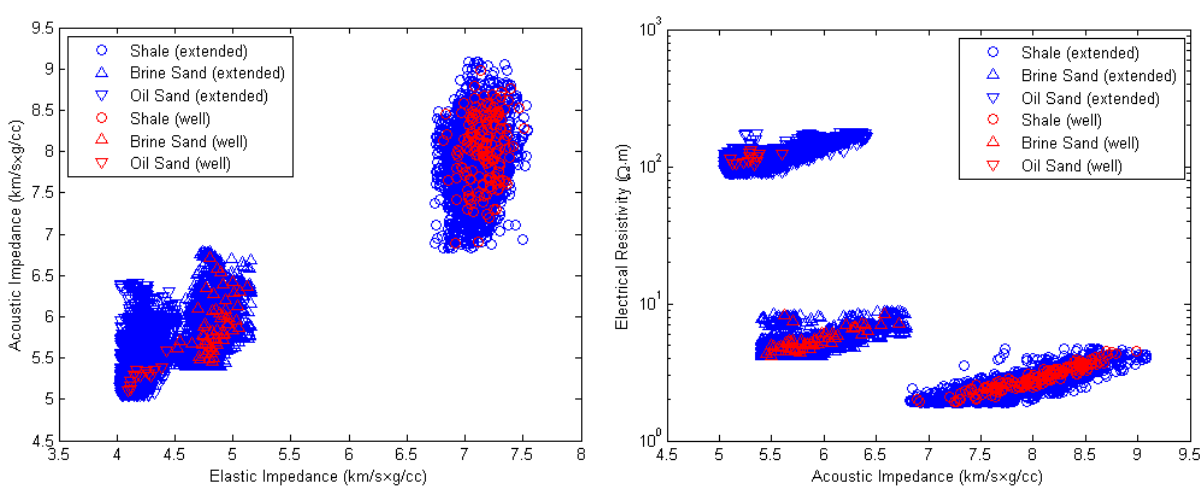

Figure 5. Seismic impedances and electrical resistivity from well logs and the extended data by rock physics modeling and Monte Carlo simulation.

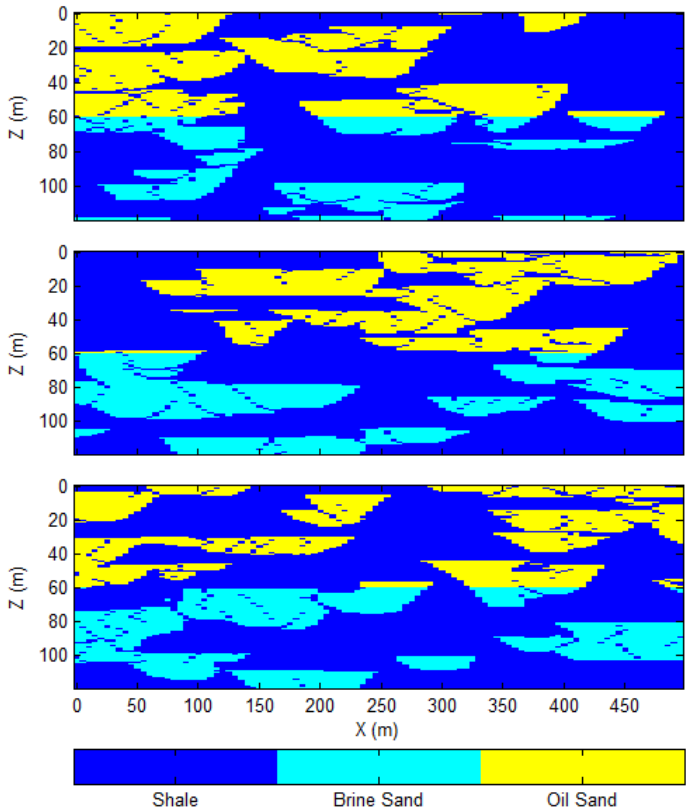

Figure 6. Realizations generated by multipoint geostatistical algorithm SNESIM.

Figure 8 compares the distributions of the extended well-scale data, the simulated field-scale data of the realizations, and the true field-scale data of the target cross section. As seen from the figure, the distribution of the field-scale data of the realizations has a lot more similarity with the distribution of the true field-scale data as compared to the extended well-scale data.

Figure 9 presents the classification results by seismic and EM data with the simulated field-scale PDF using the suggested upscaling method and seismic and EM data with the extended well-scale PDF without upscaling. The results classified by only seismic data with upscaling and only EM data with upscaling are also shown in Figure 9. All joint PDFs are estimated as nonparametric PDFs with Gaussian kernel. As shown in the figure, a lot of regions in the cross section cannot be classified when the scale differences between well logs, seismic and EM data are ignored, whereas classification result significantly improves with the developed upscaling method. In addition, this statistical integration approach represents the advantages of two different geophysical data; differentiation between shale and sand by seismic data, and between oil sand and the other facies by EM data.

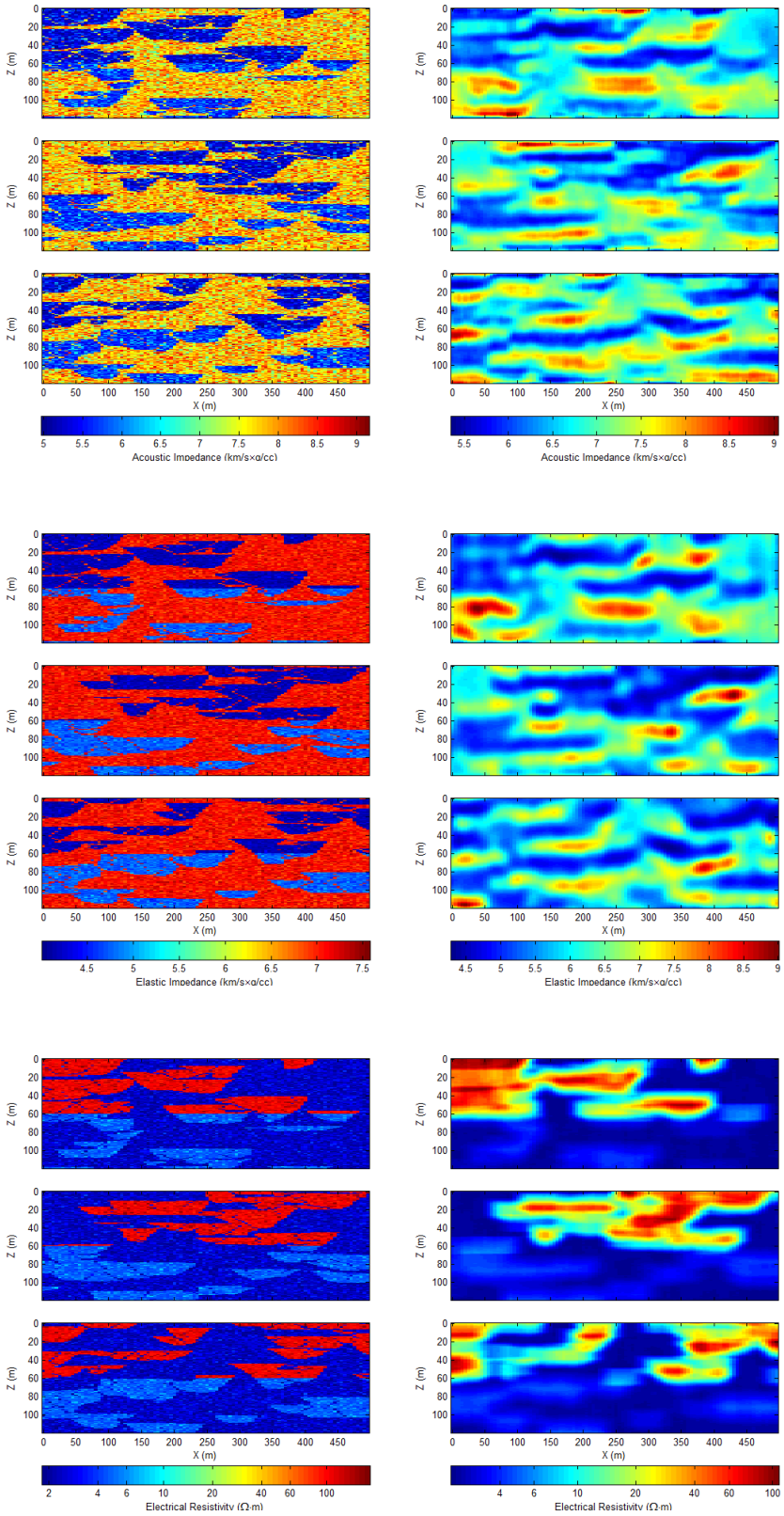

Figure 7. Well-scale (left column) and field-scale (right column) acoustic and elastic impedance and electrical resistivity of three realizations.

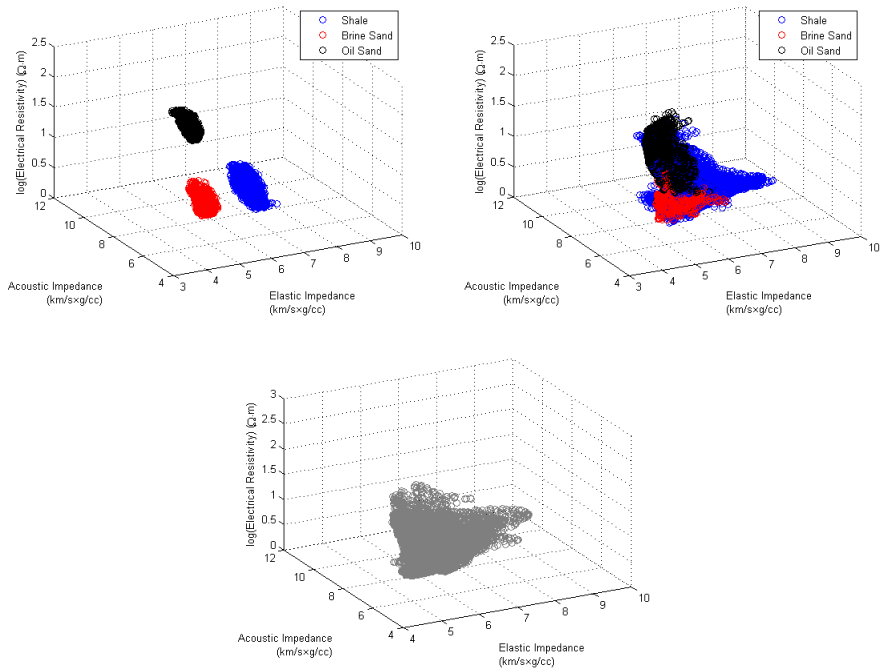

Figure 8. Distributions of the extended well log data (top-left), the simulated field-scale data of three realizations (top-right), and the true field-scale data of the target cross section (bottom). Facies are not shown for the target cross section since they are unknown in classification.

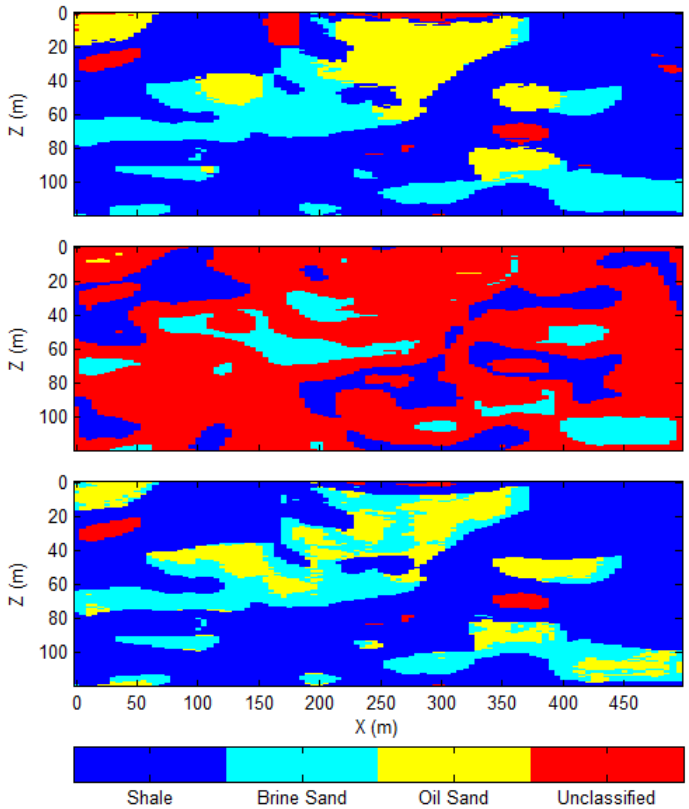

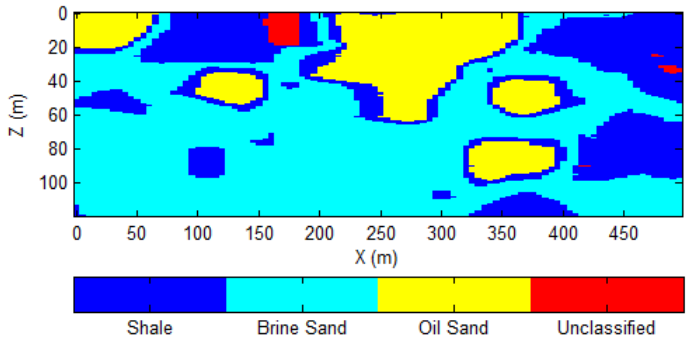

Figure 9. Classification results by seismic and EM data with the suggested upscaling method (top), seismic and EM data without upscaling (second), only seismic data with upscaling (third), and only EM data with upscaling (bottom).

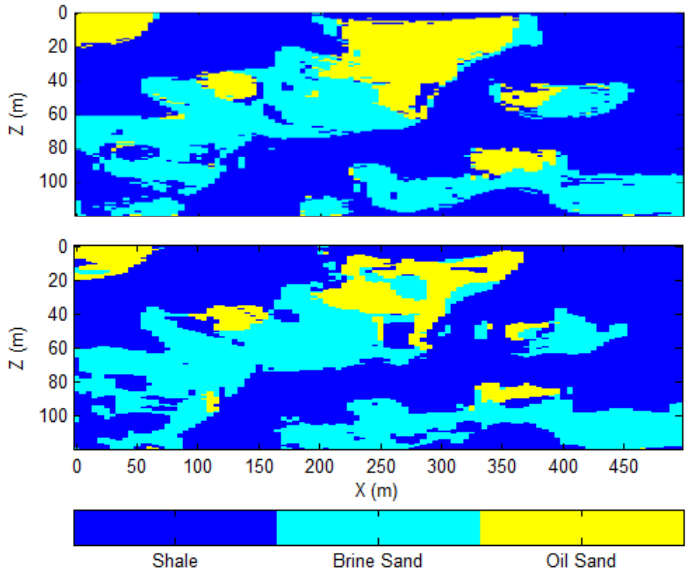

Figure 10. Classification results with time-lapse seismic and EM data with the suggested upscaling method. Seismic and EM data at two different time steps (top), and seismic and EM data at the current time step and their differences during production (bottom)

In Figure 10, classification results are presented when time-lapse seismic and EM data are incorporated into the joint PDF with the suggested upscaling method. Gaussian mixture models are used for statistical integration of time-lapse data. Better classification is achieved when seismic and EM data at the previous time step are used than the differences of those attributes between two different steps. It also provides an improved result over the one obtained from seismic and EM data at one time step (Figure 9).

Conclusions

In this research, we developed a workflow for statistical integration of time-lapse seismic and EM data with a new upscaling method. The suggested upscaling method simulates the joint PDF of field-scale seismic, EM, and reservoir properties using unconditional multi-point geostatistics. The application to facies classification in a two-dimensional cross section of a synthetic reservoir has proved that the statistical workflow can provide a new way of jointly integrating time-lapse seismic and EM data for reservoir characterization and monitoring.

The developed approach has the following advantages; 1) upscaling is conducted in a consistent way with seismic and EM forward modeling and inversion, 2) filtering can be utilized for quick estimation, 3) a few realizations are enough, 4) realizations do not have to be as large as a target reservoir, 5) time-lapse data can be incorporated into the joint PDF easily, and 6) probability maps are also obtained so they can be used for uncertainty quantification or as soft data for geostatistical algorithms.

References

Alumbaugh, D. L. and Morrison, H. F., 1995, "Theoretical and practical considerations for crosswell electromagnetic tomography assuming a cylindrical geometry": *Geophysics*, 60, 846-870.

Archie, G. E., 1942, "The electrical resistivity log as an aid in determining some reservoir characteristics": *Transactions of the AIME.*, 146, 54-62.

Avseth, P., Dvorkin, J., and Mavko, G., 2000, "Rock physics diagnostic of North Sea sands: Link between microstructure and seismic properties": *Geophysical Research Letters*, 27, 2761-2764.

Avseth, P., Mukerji, T., and Mavko, G., 2005, *Quantitative Seismic Interpretation: Applying Rock Physics Tools to Reduce Interpretation Risk*, Cambridge University Press, UK.

Castagna, J.P., Batzle, M.L., and Eastwood, R.L., 1985, **"**Relationships between compressional-wave and shear-wave velocities in clastic silicate rocks": *Geophysics*, 50,571-581.

Castagna, J.P., Batzle, M.L., and Kan, T.K., 1993, **"**Rock physics -The link between rock properties and AVO response": in *Offset-Dependent Rejlectivity - Theory and Practice of AVO Analysis,* J.P. Castagna and M. Backus, eds. *Investigations in Geophysics*, 8, Society of Exploration Geophysicists, Tulsa, Oklahoma, 135-171.

Constable, S. and Cox, C. S., 1996, "Marine controlled source electromagnetic sounding 2. The PEGASUS experiment": *Journal of Geophysics Research*, 101, 5519-5530.

Gardner, G. H. F., Gardner, L. W., and Gregory, A. R., 1974, "Formation velocity and density – the diagnostic basics for stratigraphic traps": *Geophysics*, 39, 770-780.

Gao, G., Abubakar, A., and Habashy., T. M., 2012, "Joint petrophysical inversion of electromagnetic and full-waveform seismic data", *Geophysics*, 77, 3, WA3-WA18.

Hoversten, G. M., Cassassuce, F., Gasperikova, E., Newman, G. A., Chen, J., Rubin, Y., Hou, Z., and Vasco. D., 2006, "Direct reservoir parameter estimation using joint inversion of marine seismic AVA and CSEM data": *Geophysics*, 71, 3, C1-C13.

Landrø, M., 2001, "Discrimination between pressure and fluid saturation changes from time-lapse seismic data": *Geophysics*, 66, 836-844.

Lee, J. and Mukerji, T., 2012, "The Stanford VI-E reservoir: A synthetic data set for joint seismic-EM time-lapse monitoring algorithms": 25th SCRF Annual Report, Stanford Center for Reservoir Forecasting, Stanford University, Stanford, CA.

Lumley, D., Meadows, M., Cole, S., and Adams, D., 2003, "Estimation of reservoir pressure and saturations by crossplot inversion of 4D seismic attributes": *SEG Annual Meeting*, 1513-1516.

Mukerji, T., Mavko, G., and Rio, P., 1997, "Scales of reservoir heterogeneities and impact of seismic resolution on geostatistical integration": *Mathematical Geology*, 29, 933-950.

Mukerji, T., Jørstad, A., Avseth, P., Mavko, G., and Granli, J. R., 2001, "Mapping lithofacies and pore-fluid probabilities in a North Sea reservoir: Seismic inversions and statistical rock physics": *Geophysics*, 66, 988-1001.

Strebelle, S., 2000, *Sequential Simulation Drawing Structures from Training Images*, Ph.D. thesis, Stanford University, Stanford, CA.

Strebelle, S., 2002, "Conditional simulation of complex geological structures using multiple-point statistics": *Mathematical Geology*, 34, 1-21

Tura, A. and Lumley, D, 1999, "Estimating pressure and saturation changes from time-lapse AVO data": *SEG Annual Meeting*, 1655-1658.

Waxman, M. H. and Smits, L. J. M., 1968, "Electrical conductivities in oil-bearing shaly sands": *SPE Journal*, 8, 107-122.